DCE-MRI Perfusion in Liver Disease with 3D Volumetric Coverage

Y. Huang[1], E. Brodsky[1], K. Johnson[1], E. Bultman[2], D. Horng[1,3], S. Fain[1,3], and S. Reeder[1,3]
[1]Medical Physics, University of Wisconsin Madison, Madison, WI, United States, [2]Biomedical Engineering, University of Wisconsin Madison, Madison, WI, United States, [3]Radiology, University of Wisconsin Madison, Madison, WI, United States

INTRODUCTION

Measurement of liver perfusion from dynamic contrast enhanced (DCE) MRI can be utilized for diagnosis of liver tumors and evaluation of therapy response [1]. In particular, quantitative liver perfusion measurements have potential to predict long-term tumor response to anti-angiogenic agents, based on early changes in liver tumor microvascularity. Here we investigate the feasibility of semi-quantitative metrics of contrast arrival time and area under curve (AUC) to measure perfusion in liver tumors from 3D whole-liver perfusion imaging, acquired with rapid, high spatial resolution 3D time-resolved radial perfusion imaging.

MATERIALS AND METHODS

This study complies with HIPPA and was approved by our institutional human subjects review committee. Written informed consent was collected from subjects before imaging. Subjects with focal liver lesions, including hepatocellular carcinoma (HCC) and focal nodular hyperplasia (FNH) were imaged on a 3.0T scanner (MR750, GE Healthcare) with a 32 channel abdominal coil and a 1.5T scanner (Excite HD, GE Healthcare) with an 8 channel abdominal coil respectively. After single dose injection of gadobenate dimeglumine (Bracco, Princeton, NJ), a time-resolved 4 half-echo 3D radial SPGR sequence with a coverage of whole abdomen provided a temporal resolution of 1 interleaved sub-frame/sec. Each time frame was reconstructed in real-time [2] allowing fluoroscopic monitoring of the contrast bolus. Specific scan parameters were: TR=3.8 ms, TE=0.3/0.95/1.61 ms, flip angle=12°, FOV=40 cm, BW=250 kHz, and 192 x 192 x 192 matrices. Real-time bolus tracking was used to coach sequential breath holds at 3 intervals throughout the scan: during the arterial phase of contrast arrival, portal venous phase (~ 50-70 sec), and during a delayed phase (~ 100-120 sec). Image reconstruction was performed with an auto-calibrated iterative SENSE algorithm [3]. Time-resolved image volumes at full spatial resolution (1.6x1.6x1.6mm^3) were reconstructed with an effective temporal resolution of 4s. MR data processing was performed off-line in MATLAB (Version7.5; MathWorks Inc., Cambridge, MA, USA). Mask subtracted MR signal intensity for each voxel was normalized to its baseline value. The conversion from MR signal to concentration was calculated using: $S(t) = \frac{M_0 \sin(\theta)(1-e^{-TR/T_1})}{1-\cos(\theta)e^{-TR/T_1}}$ and $\frac{1}{T_1} = \frac{1}{T_{10}} + R_1 C(t)$, where $S(t)$, M_0, θ, T_1, R_1 and $C(t)$ respectively represent MR signal at time t, equlibrium magnet, flip angle, longitudinal relaxation time, relaxation rate and contrast concentration at time t. We assumed longitudinal relaxation time before contrast, T_{10}=0.8 sec, and R_1 = 5.9 sec^{-1} mM^{-1} [4] for 3T; and T_{10}=0.6 sec, and R_1 = 7.9 sec^{-1} mM^{-1} for 1.5T. The concentration data during free breathing periods were interpolated from the adjacent breath-hold courses using a cubic spline method [5]. Prior to modeling, the concentration time curve was smoothed using a Gaussian filter along the time dimension for each voxel. The contrast arrival time was defined as the time frame with concentration at half of maximum. The AUC was calculated as the integral of concentration through the arterial uptake phase from contrast arrival time to 60 sec.

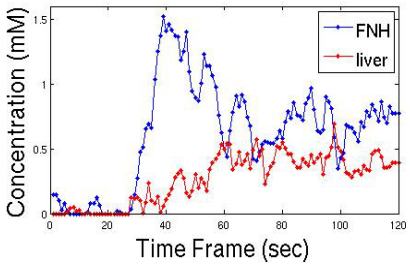

Figure 1. Concentration-time courses of a typical voxel within a FNH (blue) compared to a voxel within normal liver parenchyma (red). Note that the FNH enhances early and decays rapidly compared to adjacent parenchyma.

RESULTS AND DISCUSSION

The enhancement pattern of the FNH was characterized by early intense enhancement during the arterial phase followed by rapid equilization compared to adjacent liver parenchyma (Fig.1). Arrival time and area under the curve (AUC) for the FNH are also shown in Figure 2 in both axial and coronal planes, quantifying the perfusion of this lesion. Also note the isotropic resolution of the perfusion images and parametric measurements. Figure 2 also show an example of a small (1.9cm) HCC, demonstrating early arrival time and increased AUC. These results agree with expected liver-tumor hemodynamics since blood supply to both lesions derives from the hepatic artery instead of the portal vein, while only 20-25% of blood flow to normal liver parenchyma derives from the hepatic artery.

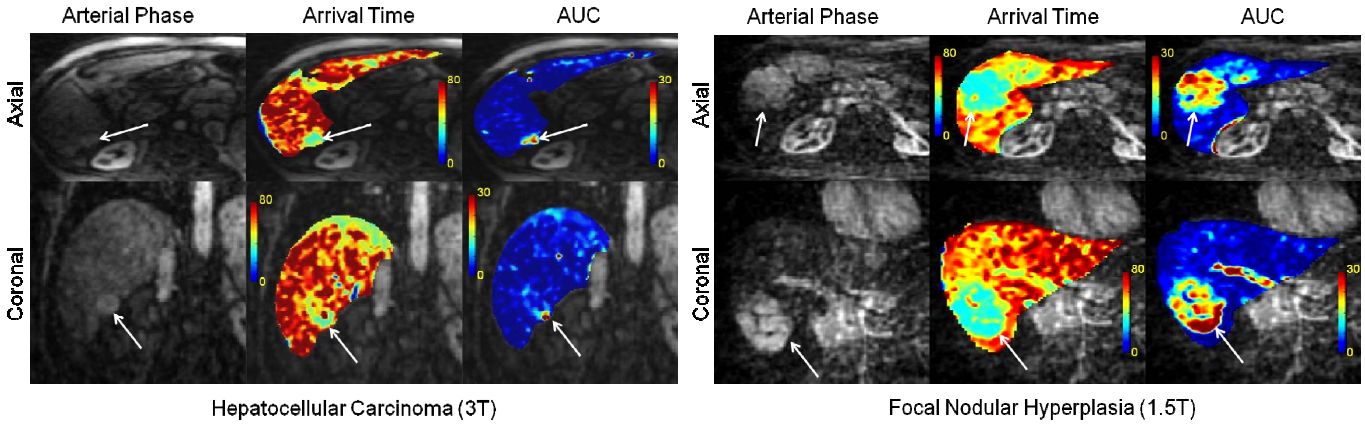

Figure 2. Arterial phase images are at time frames of 44 sec for the FNH on left and 40 sec for the HCC, left column on right. Respective parametric maps of contrast arrival and area under the curve (AUC) overlaid in color on the corresponding arterial phase images are shown in the second and third columns. The color bar for arrival time is in units of sec and AUC is in units of mM·sec. Both the FNH and HCC demonstrate early contrast arrival time and higher AUC relative to normal liver parenchyma due to higher uptake of arterial blood. The arrows in the images point out the FNH and HCC lesion locations respectively.

CONCLUSIONS

The results demonstrate the feasibility of semi-quantitative metrics of perfusion to describe tumor characteristics of liver having FNH and HCC. Future work will incoporate these metrics into an ongoing study of treatment response in liver perfusioin, and pursue quantitative perfusion modeling using a dual input model that includes separate portal vein and hepatic arterial input [6].

ACKNOWLEDGEMENTS: This work was supported by the NIH (R01DK083380, R01 DK088925 and RC1 EB010384), the Coulter Foundation, and GE Healthcare.

REFERENCES: [1]Cao et al, Med.Phys. 2006, 33(8): 3057-3062. [2] Brodsky et al, MRM 2006, 56(2):247-254. [3] Johnson KM, et al., Proc. 22nd MRA Club 2010. [4] Rumboldt et al, JMRI 2009, 29:76-767. [5] Hou et al, IEEE Trans Acoust Speech Signal Process 1978, 26 (6):508-517. [6] Materne et al, MRM 2002, 47:135-142.